

ORIGINAL ARTICLE

Quantitative super-resolution imaging of platelet degranulation reveals differential release of von Willebrand factor and von Willebrand factor propeptide from alpha-granules

Maurice Swinkels¹ | Sophie Hordijk¹ | Petra E. Bürgisser¹ |
 Johan A. Slotman² | Tom Carter³ | Frank W. G. Leebeek¹ | A. J. Gerard Jansen¹ |
 Jan Voorberg^{4,5} | Ruben Bierings¹

¹Department of Hematology, Erasmus MC, University Medical Center Rotterdam, Rotterdam, The Netherlands

²Optical Imaging Center, Department of Pathology, Erasmus MC, University Medical Center Rotterdam, Rotterdam, The Netherlands

³Molecular and Clinical Sciences Research Institute, St George's University of London, London, United Kingdom

⁴Molecular Hematology, Sanquin Research and Landsteiner Laboratory, Amsterdam University Medical Center, University of Amsterdam, Amsterdam, The Netherlands

⁵Experimental Vascular Medicine, Amsterdam University Medical Center, University of Amsterdam, Amsterdam, The Netherlands

Correspondence

Ruben Bierings, Department of Hematology, Erasmus MC, University Medical Center Rotterdam, Dr. Molewaterplein 40, 3015 GD Rotterdam, Zuid-Holland, The Netherlands.
 Email: r.bierings@erasmusmc.nl

Funding information

This study was supported by grants from the Landsteiner Stichting voor Bloedtransfusie Research (LSBR-1707 and LSBR-2005) and an European Hematology Association (EHA) Clinical Research Fellowship (to A.J.G.J.).

Abstract

Background: Von Willebrand factor (VWF) and VWF propeptide (VWFpp) are stored in eccentric nanodomains within platelet alpha-granules. VWF and VWFpp can undergo differential secretion following Weibel-Palade body exocytosis in endothelial cells; however, it is unclear if the same process occurs during platelet alpha-granule exocytosis. Using a high-throughput 3-dimensional super-resolution imaging workflow for quantification of individual platelet alpha-granule cargo, we studied alpha-granule cargo release in response to different physiological stimuli.

Objectives: To investigate how VWF and VWFpp are released from alpha-granules in response to physiological stimuli.

Methods: Platelets were activated with protease-activated receptor 1 (PAR-1) activating peptide (PAR-1 ap) or collagen-related peptide (CRP-XL). Alpha-tubulin, VWF, VWFpp, secreted protein acidic and cysteine rich (SPARC), and fibrinogen were imaged using 3-dimensional structured illumination microscopy, followed by semiautomated analysis in FIJI. Uptake of anti-VWF nanobody during degranulation was used to identify alpha-granules that partially released content.

Results: VWFpp overlapped with VWF in eccentric alpha-granule subdomains in resting platelets and showed a higher degree of overlap with VWF than SPARC or fibrinogen. Activation of PAR-1 (0.6–20 μ M PAR-1 ap) or glycoprotein VI (GPVI) (0.25–1 μ g/mL CRP-XL) signaling pathways caused a dose-dependent increase in alpha-granule exocytosis. More than 80% of alpha-granules remained positive for VWF, even at the highest agonist concentrations. In contrast, the residual fraction of alpha-granules containing VWFpp decreased in a dose-dependent manner to 23%, whereas

Manuscript handled by: David Lillicrap

Final decision: David Lillicrap, 31 March 2023

Maurice Swinkels and Sophie Hordijk contributed equally to this study.

© 2023 The Author(s). Published by Elsevier Inc. on behalf of International Society on Thrombosis and Haemostasis. This is an open access article under the CC BY license (<http://creativecommons.org/licenses/by/4.0/>).

SPARC and fibrinogen were detected in 60% to 70% of alpha-granules when stimulated with 20 μ M PAR-1 ap. Similar results were obtained using CRP-XL. Using an extracellular anti-VWF nanobody, we identified VWF in postexocytotic alpha-granules.

Conclusion: We provide evidence for differential secretion of VWF and VWFpp from individual alpha-granules.

KEYWORDS

blood platelets, exocytosis, hemostasis, secretory vesicles, von Willebrand factor

1 | INTRODUCTION

During thrombopoiesis, several types of secretory granules from bone marrow megakaryocytes are packaged into budding platelets. Release of their content enables platelets to rapidly respond to changes in their environment, such as during injury, inflammation, or when encountering pathogens. Alpha-granules are the most abundant platelet secretory organelle and contain various proteins and molecules involved in the hemostatic response [1,2]. Among these is von Willebrand factor (VWF), a key hemostatic adhesive glycoprotein whose main roles are to facilitate platelet adhesion to vascular injury sites and to stabilize coagulation factor VIII in the circulation [3]. VWF is also produced by endothelial cells and stored in Weibel-Palade bodies (WPBs), where it can be released via exocytosis following cellular activation. Circulating VWF levels in plasma are primarily maintained through basal secretion of WPBs from the endothelium [4].

Our knowledge of VWF biosynthesis primarily comes from studies utilizing endothelial cells and heterologous expression systems as cellular models. As it progresses through the secretory pathway, VWF undergoes several posttranslational processing steps, which include dimerization, glycosylation, and multimerization into long platelet-adhesive concatemers [3]. Within the acidifying milieu of the Golgi, VWF multimers condense into helical VWF tubules that lend WPBs their characteristic rod-like shape [5]. Here, a large N-terminal moiety called VWF propeptide (VWFpp) is proteolytically cleaved from the mature VWF chain. In endothelial cells, cleaved VWFpp remains noncovalently associated with VWF due to prevailing conditions in the Golgi and beyond (low pH and high Ca^{2+}), leading to its copackaging in the developing WPBs [6]. VWFpp is essential for VWF multimerization, tubulation, and WPB biogenesis [7–9] and becomes an integral part of VWF tubules *in vitro* and *in vivo* [10,11]. During exocytosis, the vesicle interior neutralizes, leading to rapid decondensation of VWF tubules [12,13] and loss of noncovalent association between VWF and VWFpp [14]. Depending on the type of exocytosis (full fusion, lingering kiss, or compound fusion) [4] and extracellular environment, VWF, VWFpp, and other WPB cargo molecules undergo divergent fates postrelease [14–17].

In platelets, VWF is zonally packaged within eccentric alpha-granule nanodomains, which also contain short VWF tubules [18–20], and can be released upon stimulus [21]. Platelets also contain

Essentials

- Activated platelets secrete hemostatic proteins from alpha-granules.
- We investigated how von Willebrand factor (VWF) and VWF propeptide (VWFpp) are released from platelet alpha-granules.
- VWF and VWFpp are localized in the same eccentric alpha-granule subdomain in resting platelets.
- VWF and VWFpp are differentially secreted from individual alpha-granules upon activation.

VWFpp [22] and are able to secrete the protein following stimulation with various agonists that induce alpha-granule release [23]. However, the organization of VWFpp in alpha-granules or its release from alpha-granules has not been documented in detail. Similar to endothelial WPBs, platelet alpha-granules can undergo single and compound exocytosis depending on the type and magnitude of stimulus [24,25]. Following activation, alpha-granule cargo such as VWF, fibrinogen, chemokines, and other mediators are not released uniformly but can vary significantly between proteins in terms of release kinetics and in the proportions that are released or retained after degranulation [26–28]. Many of these cargo proteins are nonhomogeneously distributed within alpha-granules [20,27,29–31], which has led to the hypothesis that their differential release is the result of uneven solubilization of alpha-granule cargo clusters [26]. It is unclear how these processes influence the efficiency of release of VWF and VWFpp specifically or whether VWF and VWFpp release from platelet alpha-granules is comparable to their release from endothelial cell storage organelles.

In this study, we investigated the storage and release of VWF and VWFpp in platelets using 3-dimensional structured illumination microscopy (3D-SIM). We show that VWF and VWFpp reside in a distinct alpha-granule subdomain not occupied by other alpha-granule proteins such as fibrinogen. Using quantitative 3D-SIM analysis of residual VWF and VWFpp in activated platelets, we demonstrate that VWFpp is efficiently released from platelets in a dose-dependent manner and, even at maximal activation, the bulk of VWF remains associated with platelets in postfusion structures. Our study sheds

new light on divergent outcomes of VWF and VWFpp following release from platelet alpha-granules.

2 | METHODS

2.1 | Platelet isolation

All steps were performed at room temperature (RT) unless otherwise stated. Whole blood was drawn from consenting healthy donors in citrate tubes. Washed platelets were prepared as described previously [20]. In brief, platelet-rich plasma was generated by centrifugation at $120 \times g$ for 20 minutes with low acceleration (maximum 5) and low brake (maximum 3). Platelet-rich plasma was washed once in 10% acid-citrate dextrose buffer (85 mM $\text{Na}_3\text{-citrate}$, 71 mM citric acid, and 111 mM glucose) with 111 μM prostaglandin E_1 (Sigma) and twice in washing buffer (36 mM citric acid, 103 mM NaCl, 5 mM KCl, 5 mM EDTA, and 5.6 mM glucose, pH 6.5) with 11 μM and 0 μM prostaglandin E_1 , respectively, and then resuspended at 250×10^3 platelets/ μL in assay buffer (10 mM HEPES, 140 mM NaCl, 3 mM KCl, 0.5 mM MgCl_2 , 10 mM glucose, and 0.5 mM NaHCO_3 , pH 7.4).

2.2 | Platelet activation

Washed platelets at 250×10^3 platelets/ μL were stimulated with 0 to 20 μM of protease-activated receptor 1 activating peptide (PAR-1 ap, Peptides International) or 0 to 1 $\mu\text{g}/\text{mL}$ of collagen-related peptide (CRP-XL, CambCol Labs) for 30 minutes at 37 °C. Reactions were stopped by adding 1% paraformaldehyde (final concentration) for 5 minutes and then quenched with 50 mM NH_4Cl for 5 minutes. Samples were diluted in a large volume of washing buffer, washed once, and resuspended in assay buffer at approximately $250 \times 10^3/\mu\text{L}$.

2.3 | VWF nanobody internalization assay

Washed platelets were incubated with nanobodies directed against the VWF C-terminal cystine knot domain or control nanobodies (s-VWF and R2, respectively [32]; kindly supplied by Dr Coen Maas, UMCU, The Netherlands) at a final concentration of 1 $\mu\text{g}/\text{mL}$ and were stimulated as described above. Internalized nanobodies were detected using goat anti-Alpaca IgG-AF488 (Jackson ImmunoResearch).

2.4 | Flow cytometry

Small aliquots were used for quality control of platelet activation by flow cytometry. Samples were stained with CD61-APC (BD Biosciences, 1:400) and CD62P-PE (BD Biosciences, 1:100) or with secondary anti-Alpaca IgG-AF488 (Jackson ImmunoResearch, 1:400) for 15 minutes at RT, diluted in assay buffer, and immediately read on a FACS Canto II flow cytometer (BD Biosciences). In some cases, fixed

platelets were permeabilized with 0.05% saponin before staining. Forward scatter (FSC) and side scatter (SSC) parameters were used to gate platelets and single cells, whereas single stains and isotype controls were used to determine fluorescence gating.

2.5 | Platelet seeding and immunofluorescence

Seeding and staining were performed as described previously [20]. In brief, all unique sample conditions were seeded on poly-D-lysine coated 9-mm diameter 1.5H high-precision coverslips (Marienfeld), permeabilized, and stored in PBS supplemented with 0.2% gelatin, 0.02% azide, and 0.02% saponin (PGAS). Primary and secondary antibody staining was performed in PGAS for 30 minutes at RT and washed 3 times with PGAS following incubations. The antibodies used are listed in [Supplementary Table S1](#). Finally, slides were dipped in PBS, mounted in Mowiol, and imaged within 1 week.

2.6 | Structured illumination and confocal microscopy and image analysis

All samples were imaged with SIM (Elyra PS.1, Zeiss) and confocal microscopy (SP8, Leica). Three representative fields of view were collected per donor, using 40 Z-slices with an interval of 110 nm (4.4 μm in total). Raw SIM images were reconstructed with state-of-the-art Zen Software (Zeiss). Due to very bright alpha-tubulin signals and relatively broad emission filters, crosstalk between far-red and red channels was observed, which was corrected equally in all applicable images by subtracting the far-red channel (alpha-tubulin) from the red channel. The number of 3D granular structures per platelet was separately quantified for VWF, VWFpp, secreted protein acidic and cysteine rich (SPARC), and Fbg. SIM images were analyzed through ImageJ-based processing workflows as described in detail previously [20]. In brief, individual platelets were segmented based on alpha-tubulin staining, and individual 2D and 3D granular structures were quantified based on individual staining (eg, VWF/VWFpp) by automated thresholding. Platelets in which 2D and 3D granule counts within the same channel differed by more than 15 were excluded from analysis.

For analyzing the nanobody internalization assay, images without alpha-tubulin were segmented in individual platelets based on local differences in signal intensity using in-house written macrocode (available from our <https://github.com/Clotterdam> repository). VWF+ granules were identified with 3D Object Counter [33] and converted into a mask in which the presence of VWFpp and/or VWF nanobody was measured.

2.7 | Immunoblotting

Human umbilical vein endothelial cells (grown as previously described [34]) and washed platelets were lysed in NP-40 buffer (0.5% NP-40,

150 mM NaCl, 10 mM Tris, and 5 mM EDTA, pH 8.5). Lysate samples, normalized for VWF concentration, were separated on 4% to 12% Bis-Tris NuPAGE gels (Invitrogen) under reducing conditions and transferred to 0.2 μ m nitrocellulose membranes. Membranes were probed with rabbit anti-VWF (DAKO) and rabbit anti-VWFpp [17], followed by LT680-labeled donkey anti-rabbit secondary antibodies (Li-COR). The membranes were scanned on an Odyssey scanner (Li-COR).

2.8 | Platelet secretion assay and VWF and VWFpp ELISA

Washed platelets (5.6×10^6 platelets in a final volume of 200 μ L) of 4 independent, healthy donors were stimulated with 0 to 20 μ M of PAR-1 activating peptide (Peptides International) or 0 to 1 μ g/mL collagen-related peptide (CRP-XL, CambCol Labs) for 30 minutes at 37 $^{\circ}$ C. Release and platelets were separated by centrifugation (13 000 \times g), after which platelet pellets were lysed in 50 μ L lysis buffer (1% Triton X-100, 10% glycerol, 50 mM Tris-HCl, 100 mM NaCl, and 1 mM EDTA, pH 7.4). VWF and VWFpp secretion was determined using sandwich ELISA as described earlier [35], using rabbit polyclonal anti-human VWF (DAKO; 0.5 μ g/well) or mouse monoclonal anti-human VWFpp (CLB-Pro35; 1.0 μ g/well) as coating antibodies and horseradish peroxidase (HRP)-conjugated rabbit polyclonal anti-human VWF (DAKO; 0.5 μ g/mL) or HRP-conjugated mouse monoclonal anti-human VWFpp (CLB-Pro14-3; 0.125 μ g/mL) for detection. Blocking, washing, and detection steps were performed in PBS supplemented with 0.1% Tween-20, 0.2% gelatin and 1 mM EDTA. HRP activity was measured by colorimetric detection of 3,3',5,5'-tetramethylbenzidine conversion using a Victor X4 microplate reader (Perkin Elmer). All samples were measured in duplicate in 3 different dilutions. Concentrated conditioned media from HEK293Ts stably expressing human wildtype VWF and VWFpp [36], which was calibrated against a normal plasma pool of >30 donors, was used as a standard.

2.9 | Statistical analysis

Individual stimulation conditions were compared with resting platelets by 2-way analysis of variance (ANOVA). Multiple comparisons were corrected using Sidak's multiple comparisons test. All statistical analyses were performed using GraphPad Prism (version 8). Data are presented as mean \pm 95% CI unless stated otherwise. A *P* value of <.05 was considered statistically significant.

3 | RESULTS

3.1 | VWFpp colocalizes with mature VWF in eccentric alpha-granule nanodomains

Localization of VWF and VWFpp in resting platelets was studied using 3D-SIM [20]. VWF- and VWFpp-immunoreactivity were localized to

discrete regions within the platelet (Figure 1A, Supplementary Figure S1) that were encapsulated by a P-selectin-positive membrane (Supplementary Figure S2). In the presence of SPARC and fibrinogen, these regions were identified as alpha-granules within platelet cytoplasm (Figure 1B, C). Consistent with previous ultrastructural studies [18–20,31], close inspection of our images showed that VWF and VWFpp were colocalized in a subdomain within the alpha granule (Figure 1A), whereas SPARC or fibrinogen showed a more homogenous distribution and appeared to be excluded from these VWF containing nanodomains (Figure 1B, C). Colocalization analysis confirmed striking overlap between VWF- and VWFpp-immunoreactivity within individual alpha-granules (Pearson's colocalization coefficient (PCC)_{VWFpp}: 0.521; Manders' colocalization coefficient (MCC)_{1VWFpp}: 0.590; MCC_{2VWFpp}: 0.548), (Figure 1D), whereas the overlap between VWF and SPARC or fibrinogen was lower, as expected (SPARC: PCC_{SPARC} 0.336, MCC_{1SPARC} 0.386, MCC_{2SPARC} 0.498; fibrinogen: PCC_{Fibrinogen} 0.369, MCC_{1Fibrinogen} 0.467, MCC_{2Fibrinogen} 0.571) (Figure 1D–E). In these experiments, a rabbit polyclonal antibody that specifically recognizes the cleaved and processed carboxyterminal octapeptide of VWFpp was used to visualize endogenous VWFpp [17]. Immunoblot analysis confirmed that in both endothelial and platelet lysates, this VWFpp antibody exclusively recognizes a 100 kDa protein corresponding to the size of VWFpp (Supplementary Figure S3). Probing for VWF, it was clear that platelets, unlike endothelial cells, contain only mature VWF and no detectable proVWF (Supplementary Figure S3), suggesting that proteolytic processing of proVWF into mature VWF and VWFpp is completed before or during the formation of alpha-granules in megakaryocytes and does not continue after budding of platelets. Thus, the striking overlap of VWF and VWFpp in our SIM analysis suggests that both proteins are incorporated into the same supra-molecular structures within alpha-granules and are not the result of cross-reaction of the VWFpp antibody with unprocessed proVWF.

3.2 | Differential loss of VWF and VWFpp from post-exocytotic alpha granules of activated platelets

We next investigated VWF and VWFpp secretion from individual platelet alpha granules following strong activation of PAR-1 (20 μ M PAR-1 ap) or GPVI (1 μ g/mL CRP-XL) signaling pathways to drive a high level of platelet activation and degranulation (Supplementary Figures S4 and S5). We quantified the number of VWF+ and VWFpp+ structures (alpha-granules) before and after stimulation using 3D-SIM. After PAR-1 stimulation, we observed little change in the number of VWF+ structures; however, there was a dramatic reduction in VWFpp+ structures consistent with secretion of VWFpp (Figure 2A). The remaining VWF staining was confined to P-selectin (CD62P) labeled structures, suggesting that the protein mostly resides in postexocytotic alpha-granules (Supplementary Figure S6). Stimulation with 1 μ g/mL CRP-XL gave similar results to PAR-1 ap (Figure 2C). These data suggest that VWF and VWFpp may be

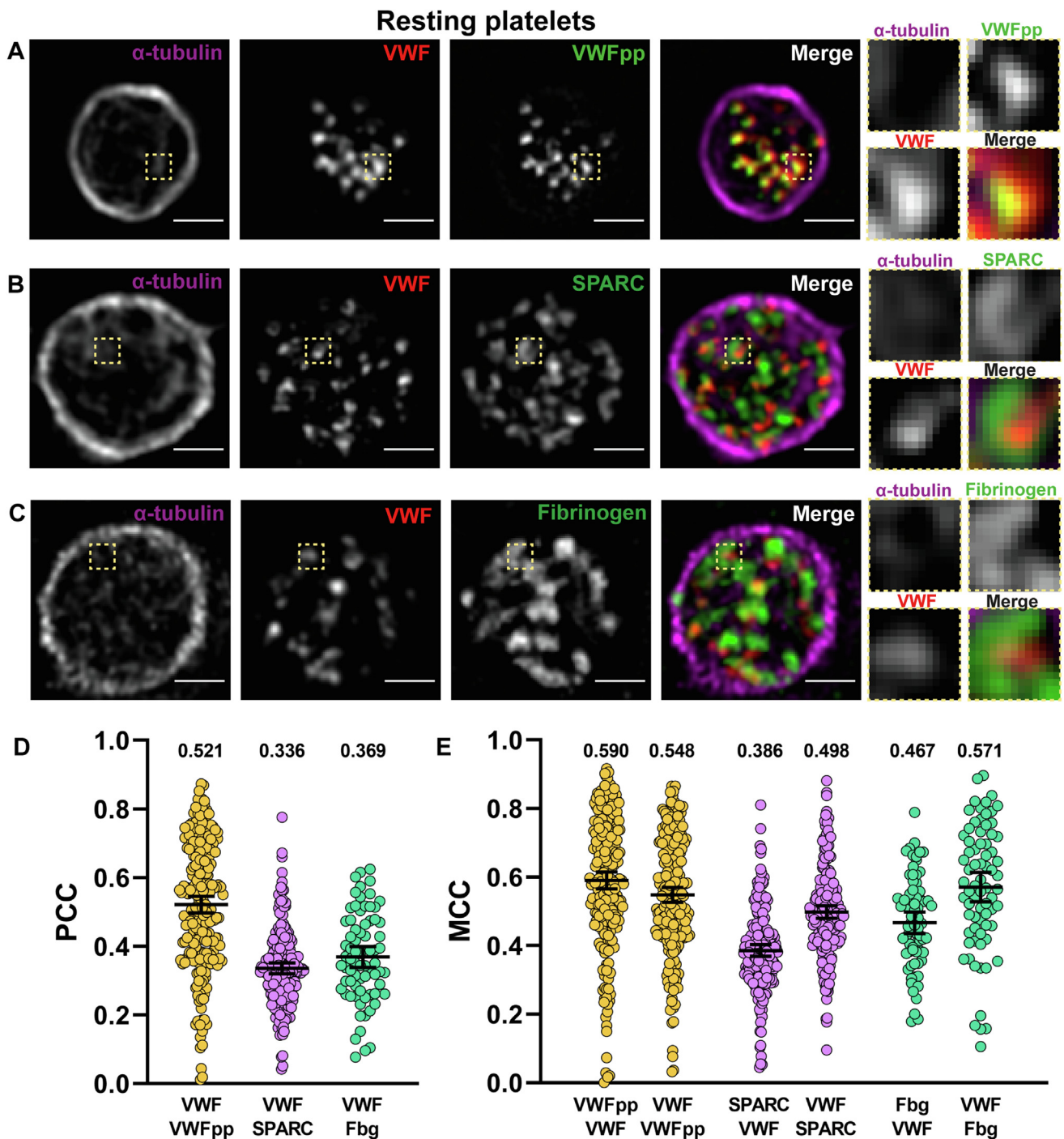


FIGURE 1 VWF and VWFpp localization in resting platelets. (A, B) Resting platelets were stained for alpha-tubulin (magenta), VWF (red, mouse monoclonal anti-VWF, CLB-RAG20), and (A) VWFpp (green), or (B) fibrinogen (green). (C) Resting platelet stained for alpha-tubulin (magenta), VWF (red, rabbit polyclonal anti-VWF, DAKO), and SPARC (green). Imaging was performed by SIM, and representative high-resolution single-plane, magnified images are shown. Areas within yellow squares that contain single granules are magnified on the right (yellow square). The scale bar represents 1 μ m. (D, E) Colocalization analysis for VWF with alpha-granule proteins VWFpp, SPARC, and fibrinogen. (D) Pearson's colocalization coefficients (PCC) and (E) pairwise Manders' colocalization coefficients (MCC) for individual platelet images (VWF-VWFpp $n = 239$, VWF-SPARC $n = 199$, VWF-Fibrinogen $n = 73$) show VWF has a higher overlap with VWFpp than with SPARC or fibrinogen. Bars indicate means with 95% CIs and mean PCC and MCC values are at the top of the graph. SIM, structured illumination microscopy; SPARC, secreted protein acidic and cysteine rich; VWF, von Willebrand factor; VWFpp, VWF propeptide.

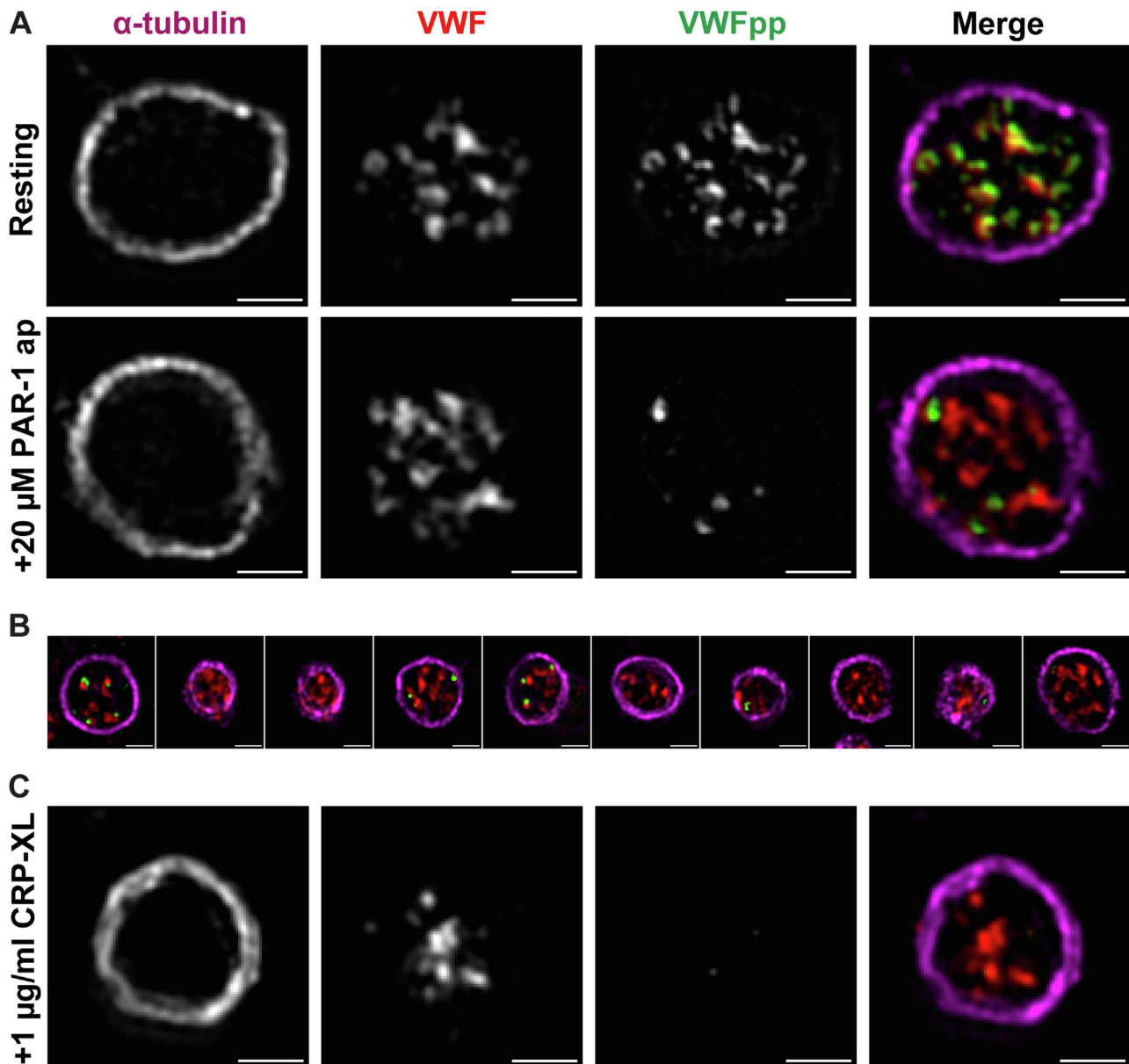


FIGURE 2 Release of VWF and VWFpp from alpha granules. Platelets were stimulated for 30 minutes with vehicle or 20 μM PAR-1 ap (A, B) or 1 $\mu\text{g}/\text{mL}$ CRP (C) and stained for alpha-tubulin (magenta), VWF (red, CLB-RAg20) and VWFpp (green). Single-plane magnified images are shown (A, C), as well as a panel of single-plane magnified images of 10 random platelets (B). The scale bar represents 1 μm . CRP, collagen-related peptide; PAR-1 ap, protease-activated receptor 1 activating peptide; VWF, von Willebrand factor; VWFpp, VWF propeptide.

differentially released by activated platelets despite their close proximity within alpha-granules in resting platelets.

Differences in VWF and VWFpp release in relation to agonist responsiveness may be explained by the large differences in size between VWF and VWFpp (VWFpp is a 100-kDa protein, whereas ultralarge VWF multimers can be in excess of 100 MDa), but we also looked at exocytosis of other alpha-granule constituents. SPARC (40 kDa) immunoreactivity was decreased more extensively than for VWF (Figure 3A); however, changes in fibrinogen (~ 340 kDa) immunoreactivity were qualitatively similar to that of VWF (Figure 3B). This would suggest that additional factors other than protein size play a role in facilitating differential agonist responsiveness of VWF vs VWFpp.

3.3 | Differential release of VWF and VWFpp relates to agonist responsiveness

Having established that strong platelet stimulation results in differential release of VWF and VWFpp, we next asked whether this phenomenon was influenced by stimulus strength. For this, we used a semiautomated quantitative workflow on 3D-SIM images [20] of platelets activated with a broad concentration range of PAR-1 and CRP-XL that partially or fully trigger alpha-granule release (Supplementary Figure S4). We found that differential release of VWF and VWFpp was apparent at all stimulus concentrations of PAR-1 ap (Figure 4A); however, it was clear that less VWFpp was retained in postexocytosis alpha-granules as the

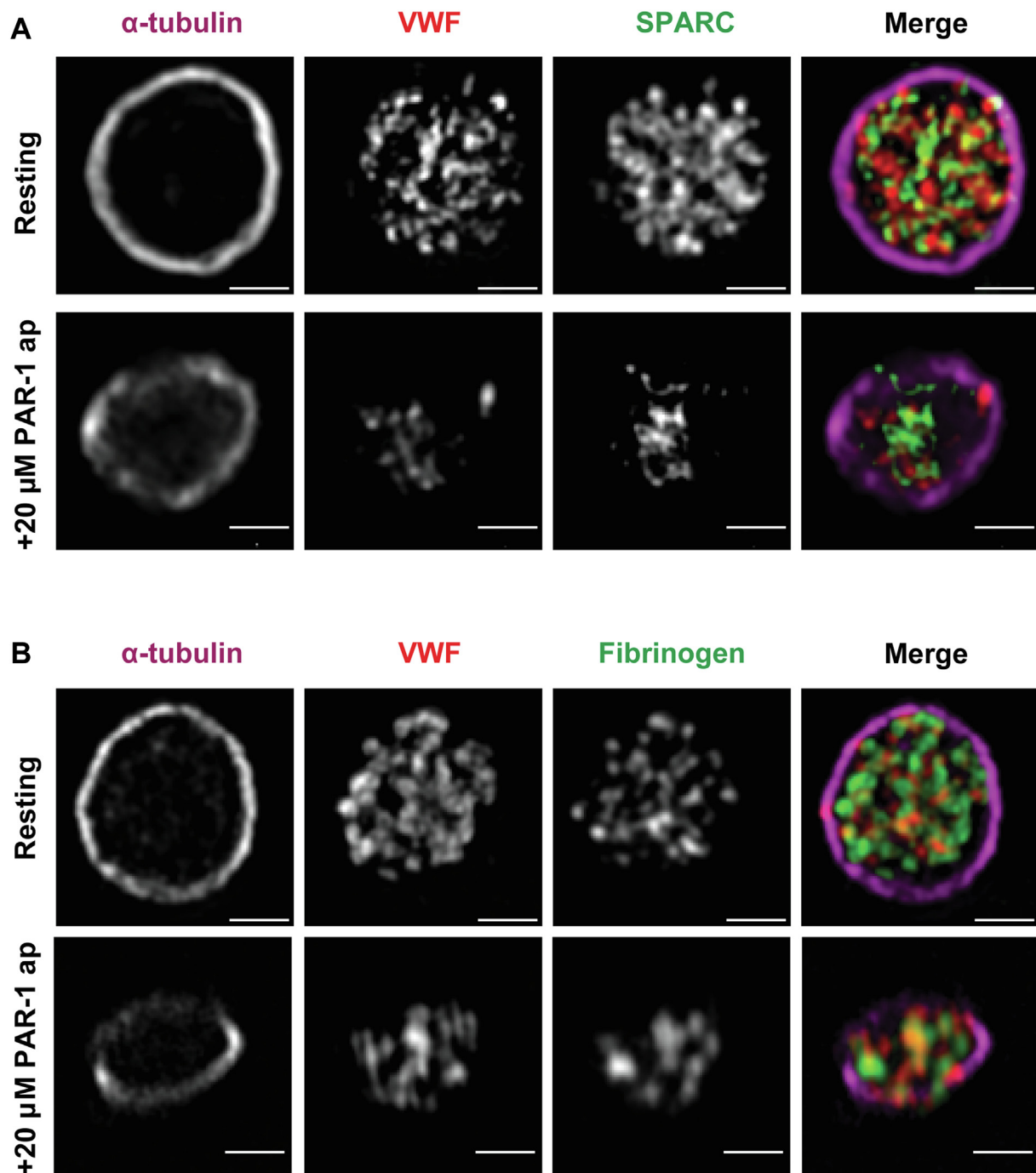


FIGURE 3 Release of SPARC and fibrinogen from alpha-granules. Platelets were stimulated with 20 μM PAR-1 and compared with resting platelets for release of alpha-granule proteins. Immunofluorescent staining for alpha-tubulin (magenta) in combination with (A) VWF (red, DAKO) and SPARC (green) or (B) VWF (red, CLB-RAG20) and fibrinogen (green). Single-plane, representative magnified images are shown. The scale bars represent 1 μm . PAR-1, protease-activated receptor 1; SPARC, secreted protein acidic and cysteine rich; VWF, von Willebrand factor; VWFpp, VWF propeptide.

stimulus strength was increased. At 0.625 μM PAR-1 ap, the fraction of VWFpp+ alpha granules was 76.8% compared with control platelets ($p < .0001$, 2-way ANOVA), and this fraction reduced to 23.4% at 20 μM PAR-1 ap ($p < .0001$, 2-way ANOVA). In contrast, for 20 μM PAR-1 ap, the fraction of VWF+ alpha granules was 80.9% of the control ($p < .0001$, 2-way ANOVA). This difference between the retention of VWF

and VWFpp was significant at all stimulus strengths. Similar findings were obtained using CRP-XL (Supplementary Figure S7A, B). Consistent with our 3D-SIM-based exocytosis assay, biochemical analysis showed that VWFpp and VWF were differentially secreted following dose-dependent activation of PAR-1 or GPVI signaling (Figure 4C, D, Supplementary Figure S7C, D).

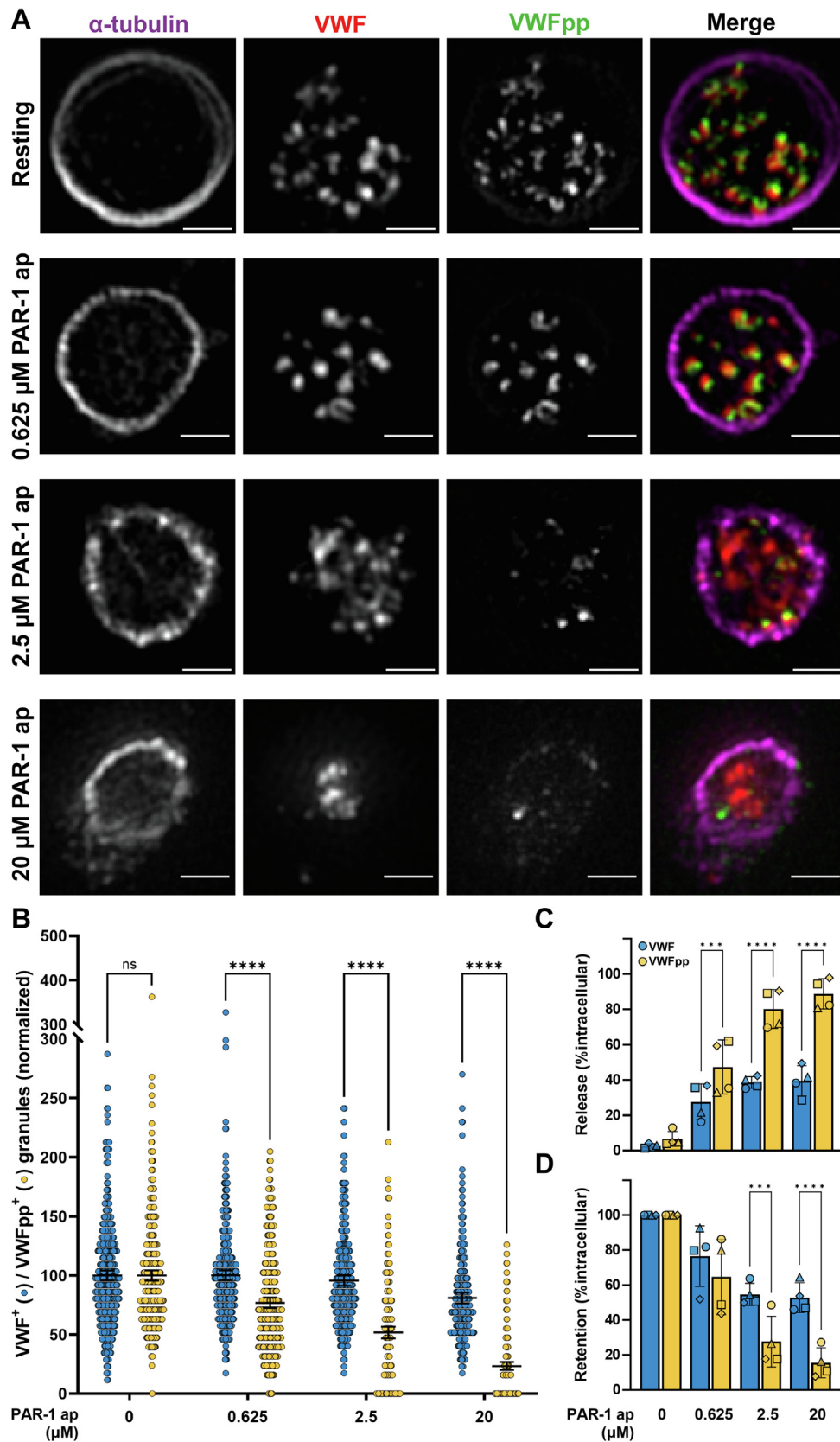


FIGURE 4 Dose-response release of VWF and VWFpp. (A) Platelets were stimulated with 0 to 20 μM PAR-1 ap and stained for alpha-tubulin (magenta), VWF (red, CLB-RAG20), and VWFpp (green). Representative single-plane, magnified images are shown. Scale bars represent 1 μm . (B) VWF and VWFpp release was assessed by quantification of residual VWF+ or VWFpp+ structures in platelets normalized to resting platelets. Counts are pooled from 3 independent, healthy donors: 0 μM PAR-1 ap $n = 435$; 0.625 μM PAR-1 ap $n = 365$; 2.5 μM PAR-1 ap

The release of SPARC and fibrinogen from alpha-granules showed a different pattern (Supplementary Figure S8). The fraction of SPARC+ or fibrinogen+ alpha granules present in stimulated platelets was reduced to 60.7% and 67.6% of the control at 20 μ M PAR-1 ap, respectively. The data illustrated that the extent of cargo release was protein specific.

In conclusion, we observed a large disparity in alpha-granule release of VWF versus VWFpp, where the former was partially retained in alpha-granules, even under strong stimulatory conditions. In contrast, VWFpp release was sensitive to lower agonist concentrations.

3.4 | Anti-VWF nanobody incorporates in postexocytotic VWF⁺ structures in degranulation-dependent manner

Finally, we wanted to study how and when individual alpha-granule structures differentially release VWF versus VWFpp. As we clearly identified granule populations that contained residual VWF but no more VWFpp, this would suggest that individual alpha-granules could perform a kiss-and-run type of exocytosis that facilitates release of selective alpha-granule cargo. To investigate this theory further, we performed a platelet degranulation experiment with an anti-VWF nanobody added in suspension, assuming that opening an alpha-granule during exocytosis would facilitate uptake of the nanobody. We found that uptake of the nanobody was directly dependent on the degree of platelet stimulation and, thus, degranulation, whereas a control R2 nanobody nonspecific for VWF did not show any signal by flow cytometry (Supplementary Figure S10A). Additionally, permeabilized platelets showed an increasingly higher mean fluorescent intensity at higher doses of PAR-1, suggesting increasing amounts of nanobody specifically inside platelets (Supplementary Figure S10A). We further confirmed this with confocal imaging, where we observed accumulation of the nanobody inside the tubulin ring at 20 μ M PAR-1 ap but not in resting platelets (Supplementary Figure S10B).

Additionally, the nanobody colocalized completely with residual VWF⁺ structures, suggesting that all VWF⁺ granules are post-exocytotic under these conditions. Together, these findings show that the uptake of the VWF nanobody is degranulation dependent. Ultimately, we analyzed individual alpha-granules that were able to take up the VWF nanobody through 3D-SIM. In accordance with flow cytometry and confocal data, we found an increasing population of VWF nanobody⁺ structures colocalizing with residual VWF that was directly related to the degree of stimulation. Most resting platelets contained granules with overlapping VWF and VWFpp signals (Figure 5A). At a low dose of PAR-1 ap (Figure 5B), only a minority of granules was strongly positive for the nanobody. However, most granules were VWF⁺ and VWFpp⁺ but revealed weak staining for the

nanobody. At a maximum dose of PAR-1 ap, we found a majority of VWF nanobody⁺ and VWF⁺ granules, but these did not contain any VWFpp (Figure 5A, B), suggesting that this content has been released during granule opening. Taken together, our findings imply that increasing doses of PAR-1 ap trigger large-scale release of VWFpp from alpha-granules, whereas VWF is partially retained in such post-exocytotic granules as evidenced by PAR-1-dependent accumulation of VWF nanobody in VWFpp⁺VWF⁺ structures. Our cumulative findings show that alpha-granules may exclusively release content like VWFpp while maintaining other cargo, like VWF, under the conditions described in our work.

4 | DISCUSSION

Important biochemical and functional differences exist between platelet and endothelial (plasma) VWF [37] that suggest dissimilarities in biosynthesis of VWF between endothelial cells and megakaryocytes: platelet VWF is composed of higher molecular weight multimers and carries different N-linked glycan structures, which makes it more resistant to proteolysis by ADAMTS13 [38] and has higher binding affinity for alphaIIb β 3 integrin [39]. In this study, we investigated the storage and exocytosis of VWF and VWFpp from platelet alpha granules through quantitative super-resolution microscopy. Our results showed that VWFpp was eccentrically localized within alpha granules in close proximity to mature VWF. In endothelial cells, VWFpp was integrated into tubules composed of helically condensed VWF multimers found within WPBs. Given that similar tubules, albeit shorter in length, have been observed in platelet alpha-granules [19], we speculated that VWFpp is similarly arranged within VWF tubules as in endothelial WPBs.

In contrast to WPBs, where the tubular arrangement of VWF is essential for its rapid and efficient release upon exocytosis, alpha-granules only released a limited amount of their VWF, even at agonist concentrations that elicited maximum surface exposure of P-selectin and led to incorporation of anti-VWF nanobody into practically all the remaining VWF-positive structures. The latter is important because it implies that all these granules have undergone a granule fusion event that generated a fusion pore in contact with the extracellular space. Additionally, we found evidence for differential release of VWFpp and VWF, showing that individual alpha-granules can preferentially release their VWFpp cargo while retaining VWF. Differential release was dependent on stimulus strength but not related to the type of agonist we used in our study. This contrasts sharply with the 1:1 stoichiometry between VWF and VWFpp released from endothelial cells [14].

What could explain the difference in secretion efficiency between VWF and VWFpp from alpha-granules? Earlier studies on the

n = 318; and 20 μ M PAR-1 ap *n* = 280 platelets. Absolute platelet counts per donor are stated in Supplementary Figure S9. The release (C) and retention (D) of VWF and VWFpp in PAR-1 ap stimulated platelets were measured by ELISA and normalized to resting intracellular content. Statistical analysis was performed by 2-way ANOVA with Sidak's multiple comparisons test at significance levels of ****p* < .001 and *****p* < .0001. The bars show means with 95% CIs. PAR-1 ap, protease-activated receptor 1 activating peptide; VWF, von Willebrand factor; VWFpp, VWF propeptide.

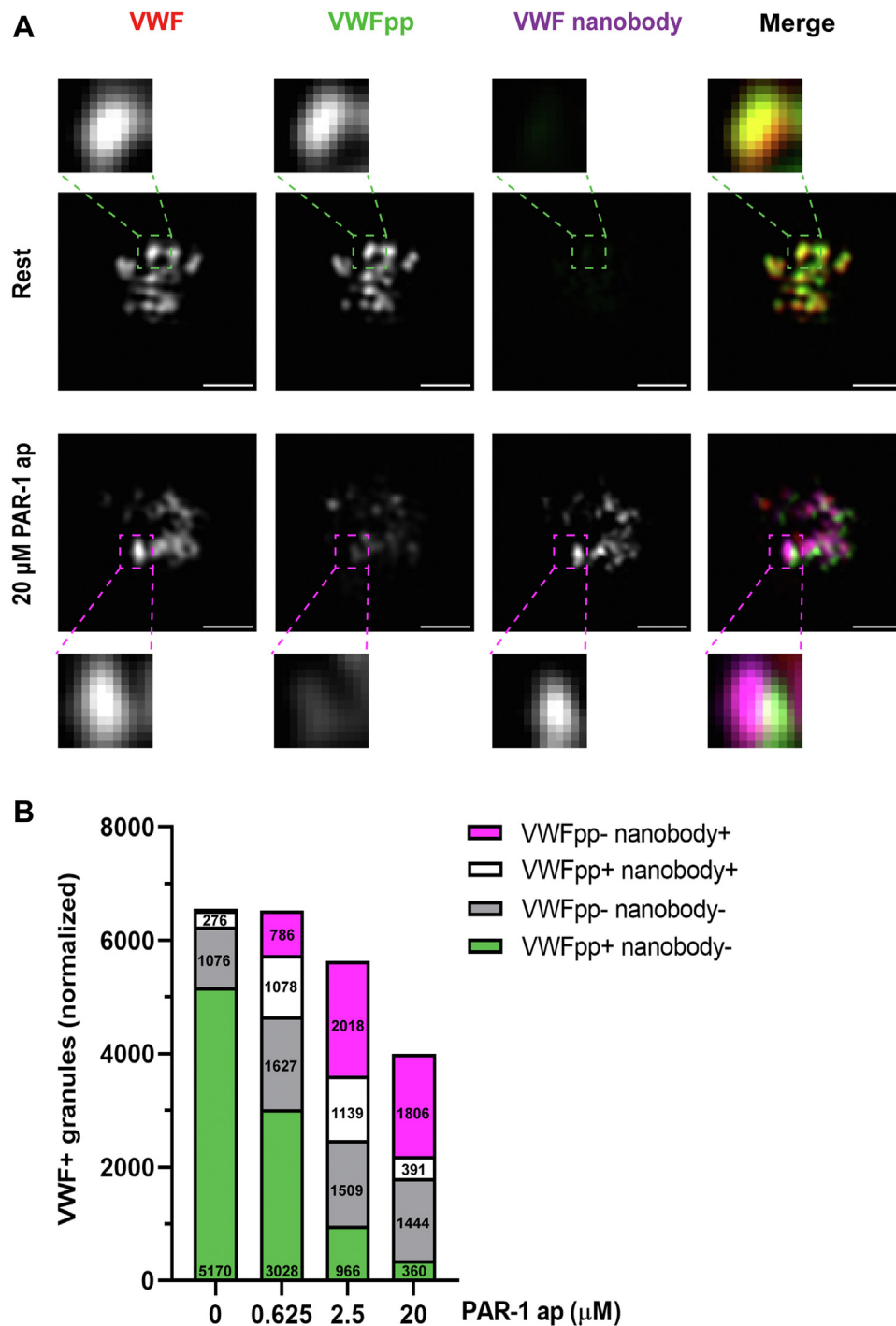


FIGURE 5 SIM analysis of VWF nanobody uptake during alpha granule release. (A) Platelets were stimulated with 0 to 20 μ M of PAR-1 ap in the presence of 1 μ g/mL VWF nanobody (magenta) and stained for VWF (red, CLB-RAg20) and VWFpp (green). A single-plane, representative magnified image of granule content of a resting and maximum stimulated platelet. The magnified region shows single granule content. Scale bar represents 1 μ m. (B) Granule populations of positive VWF/VWFpp/VWF-nanobodies were quantified for each stimulus condition. Platelet counts are pooled from 4 independent, healthy donors: 0 μ M PAR-1 ap $n = 835$; 0.625 μ M PAR-1 ap $n = 696$; 2.5 μ M PAR-1 ap $n = 748$; and 20 μ M PAR-1 ap $n = 620$ platelets. Granule counts were normalized to the number of platelets that were analyzed and indicated within their respective boxes within the stacked bar graph. PAR-1 ap, protease-activated receptor 1 activating peptide; SIM, structured illumination microscopy; VWF, von Willebrand factor; VWFpp, VWF propeptide.

organization and exocytosis of different types of alpha-granule cargo have resulted in several models of how platelets can (differentially) release their content. Based on the localization of several alpha-

granule cargo proteins, including VWF, fibrinogen, and several proangiogenic and antiangiogenic mediators, it was postulated that subpopulations of alpha-granules exist based on the inclusion of

cargo with opposing functions [29,40]. Preferential mobilization of one of these subpopulations by specific agonists would then lead to differential release of distinct functional classes of alpha-granule cargo, allowing platelets to direct their secretory response in a context-specific manner. However, this hypothesis was significantly challenged by quantitative, high-resolution imaging showing that alpha-granule cargo is stochastically packaged in alpha granules but segregated within subdomains of the granule matrix [27,30,31]. Kinetic release studies also showed little evidence of specific alpha-granule subpopulations but instead identified 3 classes of cargo release based on their rate constants (fast, intermediate, and slow) in which alpha-granule cargo distribution is random [26]. Several non-mutually exclusive mechanisms have been proposed that can achieve differential release of VWF and other cargo from the same granule, such as exocytotic fusion mode (direct vs lingering kiss vs compound fusion) [41,42] from WPBs, or differences in cargo solubilization such as the polar release of nonhomogeneously distributed cargo from one side of the alpha granule [26]. The nearly perfect overlap between VWF and VWFpp that we observed in resting platelets (Figures 1 and 2, Supplementary Figure S2) suggests that both proteins are localized in the same alpha granules and occupy the same granule subdomains, which rules out that the differences in their release were reflective of granule subpopulations or could have been the result of polar release of cargo from one end of the granule. Differential release through premature closure of the fusion pore, such as in lingering kiss exocytosis [41], is also unlikely to serve as an explanation since the size of VWFpp (~100 kDa) would require the fusion pore to fully expand before release. Indeed, we did not find an obvious correlation between releasability and size, as SPARC (40 kDa) was less sensitive to low-concentration stimulation and achieved lower maximal release than VWFpp (Supplementary Figure S8).

In line with previous reports by others [25,43], we frequently observed a clustering of VWF-positive structures in the central area of activated platelets that were negative for VWFpp, especially at higher agonist concentrations (Figure 4, Supplementary Figure S7). In some cases, a continuous P-selectin staining enveloping several VWF-positive structures (Supplementary Figure S6) was present, reminiscent of several alpha granules that had engaged in compound fusion. This exocytotic fusion mode likely poses no obstacle for VWFpp but does not favor the release of bulky, multimeric cargo, such as VWF, for instance by preventing the orderly unfurling of VWF tubules [42,44]. This may indirectly also relate to differences in solubility of VWF and VWFpp, such as previously observed during loss from the cell surface of endothelial cells following release from WPBs [15]. As a result, VWF remains stuck in postfusion alpha granules, whereas VWFpp is efficiently released.

While traces of VWFpp may stick to the D'D3 region of VWF postrelease [45], it is likely that after exocytosis, its extracellular course is primarily VWF-independent, as attested by the large difference in plasma survival between VWF and VWFpp [46]. However, despite the well-documented pleiotropic roles of VWF, the biological function of extracellular VWFpp remains unclear. Several *in vitro*

studies have demonstrated that bovine VWFpp can bind to collagen type I [47], and this interaction can block collagen-induced platelet aggregation [48]. VWFpp also contains an arginine-glycine-aspartic acid (RGD) sequence, a motif that can serve as a ligand for a subfamily of integrins that contain alpha-5, alpha-8, alpha-V, and alpha-IIb subunits. The VWFpp RGD motif is not strongly conserved between species [49]; the integrin receptor for this site has not been identified, and its significance remains uncertain as the RGD sequence appears unfavorably arranged within the native conformation to support adhesive interactions [48]. Bovine VWFpp can bind alpha4beta1 and alpha9beta1 integrins, which are expressed on lymphocytes, monocytes, and neutrophils via a sequence within the VWD2 domain conserved in humans [50–52]. Another ligand for these integrins, coagulation factor FXIII, has been shown to crosslink VWFpp to the extracellular matrix protein laminin [52–54]. Focused release of VWFpp from degranulating platelets during initial thrombus formation and incorporation in the adhesive surface via laminin and collagen possibly provides a mechanism to influence the adhesive properties of the exposed extracellular matrix and direct hemostatic and immune responses following vascular injury. Recent reports have emerged that VWFpp can contribute to platelet adhesion to collagen surfaces and enhance thrombus mass in a glycan-dependent manner [55], and in a murine model of deep vein thrombosis, VWFpp incorporates in venous thrombi near regions of active thrombus formation [56].

We have recently shown that platelet factor 4 (PF4) levels in plasma are positively correlated with the current severity of bleeding phenotype in patients with VWD type 1 [57]. PF4 is a chemokine that is mainly produced by megakaryocytes and stored in platelet alpha-granules, which means that systemic PF4 levels are reflective of platelet degranulation. One possible explanation for the observed association with bleeding severity in this group is that apart from a quantitative deficiency of VWF in plasma, hemostatic contribution of platelets is impaired by premature release of alpha-granules. This could lead to insufficient delivery of their hemostatic content, such as platelet VWF and other alpha-granule cargo, to sites of vascular injury. A number of studies have focused on the role of platelet-derived VWF in hemostasis [58–62]. Patients with mild and severe circulating VWF deficiencies with residual platelet VWF show a milder clinical phenotype [20,63]. Platelet VWF has also been reported to be important for DDAVP-related amelioration of bleeding times in subgroups of patients with type 1 VWD [64]. Together, this leads to the notion that release of platelet VWF helps to establish hemostasis in these patients. Our data suggest that following activation, most mature VWF remains within the platelets, not supporting any interactions that can contribute to the hemostatic functions of platelets, such as adhesion or aggregation. This is in contrast to its proteolytic cleavage product VWFpp, which is efficiently released from platelet alpha-granules following activation and has its own capabilities to interact with components of the extracellular matrix, cellular adhesion receptors, and the thrombus. The question thus arises how much of the perceived role of platelet VWF in hemostasis can be attributed to mature VWF and how much (if not more) is actually

dependent on VWFpp. More studies that focus on the extracellular role(s) of VWFpp, from endothelial and platelet origin, are urgently needed.

ACKNOWLEDGMENTS

We thank Dr Coen Maas (University Medical Center Utrecht, The Netherlands) for the generous supply of Alpaca anti-VWF C-terminal cystine knot nanobodies. We thank Titus Lemmens (Maastricht University Medical Center+, The Netherlands) for stimulating discussion and experimental assistance.

AUTHOR CONTRIBUTIONS

M.S., S.H., P.E.B., J.A.S., and R.B. performed experiments and analyzed the data. T.C. and F.W.G.L. provided essential reagents and expertise. M.S., S.H., A.J.G.J., J.V., and R.B. designed the research and wrote the paper. All authors critically revised and approved the final version of the manuscript.



DECLARATION OF COMPETING INTERESTS

F.W.G.L. received research support from CSL Behring, Takeda, uniQure, and Sobi and is a consultant for uniQure, Biomarin, CSL Behring, and Takeda, of which the fees go to the institute. He was a DSMB member for a study sponsored by Roche. A.J.G.J. received speaker fees and travel cost payments from 3SBio, Amgen, and Novartis, is on the international advisory board at Novartis, and received research support from CSL Behring, Principia, and Argenx. None of the other authors have conflicts of interest to declare.

TWITTER

Maurice Swinkels  @MauriceSwinkels

Sophie Hordijk  @sophiehordijk

Ruben Bierings  @rbierings;  @clotterdam

REFERENCES

- [1] Yadav S, Storrie B. The cellular basis of platelet secretion: emerging structure/function relationships. *Platelets*. 2017;28:108–18.
- [2] Karampini E, Bierings R, Voorberg J. Orchestration of primary hemostasis by platelet and endothelial lysosome-related organelles. *Arterioscler Thromb Vasc Biol*. 2020;40:1441–53.
- [3] Springer TA. Von Willebrand factor, Jedi knight of the bloodstream. *Blood*. 2014;124:1412–26.
- [4] Schillemans M, Karampini E, Kat M, Bierings R. Exocytosis of Weibel-Palade bodies: how to unpack a vascular emergency kit. *J Thromb Haemost*. 2019;17:6–18.
- [5] Valentijn KM, Sadler JE, Valentijn JA, Voorberg J, Eikenboom J. Functional architecture of Weibel-Palade bodies. *Blood*. 2011;117:5033–43.
- [6] Vischer U, Wagner D. Von Willebrand factor proteolytic processing and multimerization precede the formation of Weibel-Palade bodies. *Blood*. 1994;83:3536–44.
- [7] Wagner DD, Saffari-pour S, Bonfanti R, Sadler JE, Cramer EM, Chapman B, Mayadas TN. Induction of specific storage organelles by von Willebrand factor propeptide. *Cell*. 1991;64:403–13.
- [8] Voorberg J, Fontijn R, Calafat J, Janssen H, van Mourik JA, Pannekoek H. Biogenesis of von Willebrand factor-containing organelles in heterologous transfected CV-1 cells. *EMBO J*. 1993;12:749–58.
- [9] Haberichter SL, Fahs SA, Montgomery RR. Von Willebrand factor storage and multimerization: 2 independent intracellular processes. *Blood*. 2000;96:1808–15.
- [10] Huang R-H, Wang Y, Roth R, Yu X, Purvis AR, Heuser JE, Egelman EH, Sadler JE. Assembly of Weibel Palade body-like tubules from N-terminal domains of von Willebrand factor. *Proc Natl Acad Sci U S A*. 2008;105:482–7.
- [11] Berriman JA, Li S, Hewlett LJ, Wasilewski S, Kiskin FN, Carter T, Hannah MJ, Rosenthal PB. Structural organization of Weibel-Palade bodies revealed by cryo-EM of vitrified endothelial cells. *Proc Natl Acad Sci U S A*. 2009;106:17407–12.
- [12] Michaux G, Abbitt KB, Collinson LM, Haberichter SL, Norman KE, Cutler DF. The physiological function of von Willebrand's factor depends on its tubular storage in endothelial Weibel-Palade bodies. *Dev Cell*. 2006;10:223–32.
- [13] Conte IL, Cookson E, Hellen N, Bierings R, Mashanov G, Carter T. Is there more than one way to unpack a Weibel-Palade body? *Blood*. 2015;126:2165–7.
- [14] Wagner DD, Fay PJ, Sporn LA, Sinha S, Lawrence SO, Marder VJ. Divergent fates of von Willebrand factor and its propeptide (von Willebrand antigen II) after secretion from endothelial cells. *Proc Natl Acad Sci U S A*. 1987;84:1955–9.
- [15] Hannah MJ, Skehel P, Erent M, Knipe L, Ogden D, Carter T. Differential kinetics of cell surface loss of von Willebrand factor and its propeptide after secretion from Weibel-Palade bodies in living human endothelial cells. *J Biol Chem*. 2005;280:22827–30.
- [16] Babich V, Knipe L, Hewlett L, Meli A, Dempster J, Hannah MJ, Carter T. Differential effect of extracellular acidosis on the release and dispersal of soluble and membrane proteins secreted from the Weibel-Palade body. *J Biol Chem*. 2009;284:12459–68.
- [17] Hewlett L, Zupančič G, Mashanov G, Knipe L, Ogden D, Hannah MJ, Carter T. Temperature-dependence of Weibel-Palade body exocytosis and cell surface dispersal of von Willebrand factor and its propeptide. *PLoS One*. 2011;6:e27314.
- [18] Cramer E, Meyer D, le Menn R, Breton-Gorius J. Eccentric localization of von Willebrand factor in an internal structure of platelet alpha-granule resembling that of Weibel-Palade bodies. *Blood*. 1985;66:710–3.
- [19] van Nispen tot Pannerden H, de Haas F, Geerts W, Posthuma G, van Dijk S, Heijnen HFG. The platelet interior revisited: electron tomography reveals tubular α -granule subtypes. *Blood*. 2010;116:1147–56.
- [20] Swinkels M, Atiq F, Bürgisser PE, Slotman JA, Houtsmuller AB, de Heus C, Klumperman J, Leebeek FWG, Voorberg J, Jansen AJG, Bierings R. Quantitative 3D microscopy highlights altered von Willebrand factor α -granule storage in patients with von Willebrand disease with distinct pathogenic mechanisms. *Res Pract Thromb Haemost*. 2021;5:e12595.
- [21] Koutts J, Walsh PN, Plow EF, Fenton JW II, Bouma BN, Zimmerman TS. Active release of human platelet factor VIII-related antigen by adenosine diphosphate, collagen, and thrombin. *J Clin Invest*. 1978;62:1255–63.
- [22] Montgomery RR, Zimmerman TS. Von Willebrand's disease antigen II. A new plasma and platelet antigen deficient in severe von Willebrand's disease. *J Clin Invest*. 1978;61:1498–507.
- [23] Scott J, Montgomery R. Platelet von Willebrand's antigen II: active release by aggregating agents and a marker of platelet release reaction in vivo. *Blood*. 1981;58:1075–80.
- [24] Morgenstern E, Neumann K, Patscheke H. The exocytosis of human blood platelets. A fast freezing and freeze-substitution analysis. *Eur J Cell Biol*. 1987;43:273–82.
- [25] Eckly A, Rinckel J-Y, Proamer F, Ulas N, Joshi S, Whiteheart SW, Gachet C. Respective contributions of single and compound granule fusion to secretion by activated platelets. *Blood*. 2016;128:2538–49.

- [26] Jonnalagadda D, Izu LT, Whiteheart SW. Platelet secretion is kinetically heterogeneous in an agonist-responsive manner. *Blood*. 2012;120:5209–16.
- [27] Sehgal S, Storrie B. Evidence that differential packaging of the major platelet granule proteins von Willebrand factor and fibrinogen can support their differential release. *J Thromb Haemost*. 2007;5:2009–16.
- [28] Wijten P, van Holten T, Woo LL, Bleijerveld OB, Roest M, Heck AJR, Scholten A. High precision platelet releasate definition by quantitative reversed protein profiling—brief report. *Arterioscler Thromb Vasc Biol*. 2013;33:1635–8.
- [29] Italiano JE, Richardson JL, Patel-Hett S, Battinelli E, Zaslavsky A, Short S, Ryeom S, Folkman J, Klement GL. Angiogenesis is regulated by a novel mechanism: pro- and antiangiogenic proteins are organized into separate platelet α granules and differentially released. *Blood*. 2008;111:1227–33.
- [30] Kamykowski J, Carlton P, Sehgal S, Storrie B. Quantitative immunofluorescence mapping reveals little functional coclustering of proteins within platelet α -granules. *Blood*. 2011;118:1370–3.
- [31] Pokrovskaya ID, Yadav S, Rao A, McBride E, Kamykowski JA, Zhang G, Aronova MA, Leapman RD, Storrie B. 3D ultrastructural analysis of α -granule, dense granule, mitochondria, and canalicular system arrangement in resting human platelets. *Pract Thromb Haemost*. 2020;4:72–85.
- [32] de Maat S, Clark CC, Barendrecht AD, Smits S, van Kleef ND, El Otmani H, Waning M, van Moorsel M, Szardenings M, Delaroye N, Vercruyse K, Urbanus RT, Sebastian S, Lenting PJ, Hagemeyer C, Renné T, Vanhoorelbeke K, Tersteeg C, Maas C. Microlyse: a thrombolytic agent that targets VWF for clearance of microvascular thrombosis. *Blood*. 2022;139:597–607.
- [33] Bolte S, Cordelières FP. A guided tour into subcellular colocalization analysis in light microscopy. *J Microsc*. 2006;224:213–32.
- [34] Karampini E, Bürgisser PE, Olins J, Mulder AA, Jost CR, Geerts D, Voorberg J, Bierings R. Sec22b determines Weibel-Palade body length by controlling anterograde ER-Golgi transport. *Haematologica*. 2021;106:1138–47.
- [35] Schillemans M, Karampini E, van den Eshof BL, Gangaev A, Hofman M, van Breevoort D, Meems H, Janssen H, Mulder AA, Jost CR, Escher JC, Adam R, Carter T, Koster AJ, van den Biggelaar M, Voorberg J, Bierings R. Weibel-Palade body localized syntaxin-3 modulates von Willebrand factor secretion from endothelial cells. *Arterioscler Thromb Vasc Biol*. 2018;38:1549–61.
- [36] van den Biggelaar M, Bierings R, Storm G, Voorberg J, Mertens K. Requirements for cellular co-trafficking of factor VIII and von Willebrand factor to Weibel-Palade bodies. *J Thromb Haemost*. 2007;5:2235–42.
- [37] McGrath RT, McRae E, Smith OP, O'Donnell JS. Platelet von Willebrand factor—structure, function and biological importance. *Br J Haematol*. 2010;148:834–43.
- [38] McGrath RT, van den Biggelaar M, Byrne B, O'Sullivan JM, Rawley O, O'Kennedy R, Voorberg J, Preston RJS, O'Donnell JS. Altered glycosylation of platelet-derived von Willebrand factor confers resistance to ADAMTS13 proteolysis. *Blood*. 2013;122:4107–10.
- [39] Williams SB, McKeown LP, Krutzsch H, Hansmann K, Gralnick HR. Purification and characterization of human platelet von Willebrand factor. *Br J Haematol*. 1994;88:582–91.
- [40] Battinelli EM, Thon JN, Okazaki R, Peters CG, Vijey P, Wilkie AR, Noetzi LJ, Flaumenhaft R, Italiano JE. Megakaryocytes package contents into separate α -granules that are differentially distributed in platelets. *Blood Adv*. 2019;3:3092–8.
- [41] Babich V, Meli A, Knipe L, Dempster JE, Skehel P, Hannah MJ, Carter T. Selective release of molecules from Weibel-Palade bodies during a lingering kiss. *Blood*. 2008;111:5282–90.
- [42] Stevenson NL, White IJ, McCormack JJ, Robinson C, Cutler DF, Nightingale TD. Clathrin-mediated post-fusion membrane retrieval influences the exocytic mode of endothelial Weibel-Palade bodies. *J Cell Sci*. 2017;130:2591–605.
- [43] Stenberg PE, Shuman MA, Levine SP, Bainton DF. Redistribution of alpha-granules and their contents in thrombin-stimulated platelets. *J Cell Biol*. 1984;98:748–60.
- [44] Mourik MJ, Valentijn Ja, Voorberg J, Koster AJ, Valentijn KM, Eikenboom J. von Willebrand factor remodeling during exocytosis from vascular endothelial cells. *J Thromb Haemost*. 2013;11:2009–19.
- [45] Madabhushi SR, Shang C, Dayananda KM, Rittenhouse-Olson K, Murphy M, Ryan TE, Montgomery RR, Neelamegham S. von Willebrand factor (VWF) propeptide binding to VWF D'D3 domain attenuates platelet activation and adhesion. *Blood*. 2012;119:4769–78.
- [46] van Mourik JA, Boertjes R, Huisveld IA, Fijnvandraat K, Pajkrt D, van Genderen PJ, Fijnheer R. Von Willebrand factor propeptide in vascular disorders: a tool to distinguish between acute and chronic endothelial cell perturbation. *Blood*. 1999;94:179–85.
- [47] Takagi J, Kasahara K, Sekiya F, Inada Y, Saito Y. A collagen-binding glycoprotein from bovine platelets is identical to propolypeptide of von Willebrand factor. *J Biol Chem*. 1989;264:10425–30.
- [48] Takagi J, Sekiya F, Kasahara K, Inada Y, Saito Y. Inhibition of platelet-collagen interaction by propolypeptide of von Willebrand factor. *J Biol Chem*. 1989;264:6017–20.
- [49] Janel N, Ribba A-S, Chérel G, Kerbiriou-Nabias D, Meyer D. Primary structure of the propeptide and factor VIII-binding domain of bovine von Willebrand factor. *Biochim Biophys Acta*. 1997;1339:4–8.
- [50] Takagi J, Sudo Y, Saito T, Saito Y. Beta1-integrin-mediated adhesion of melanoma cells to the propolypeptide of von Willebrand factor. *Eur J Biochem*. 1994;222:861–8.
- [51] Isobe T, Hisaoka T, Shimizu A, Okuno M, Aimoto S, Takada Y, Saito Y, Takagi J. Propolypeptide of von Willebrand factor is a novel ligand for very late antigen-4 integrin. *J Biol Chem*. 1997;272:8447–53.
- [52] Takahashi H, Isobe T, Horibe S, Takagi J, Yokosaki Y, Sheppard D, Saito Y. Tissue transglutaminase, coagulation factor XIII, and the pro-polypeptide of von Willebrand factor are all ligands for the integrins $\alpha 9 \beta 1$ and $\alpha 4 \beta 1$. *J Biol Chem*. 2000;275:23589–95.
- [53] Usui T, Takagi J, Saito Y. Propolypeptide of von Willebrand factor serves as a substrate for factor XIIIa and is cross-linked to laminin. *J Biol Chem*. 1993;268:12311–6.
- [54] Takagi J, Aoyama T, Ueki S, Ohba H, Saito Y, Lorand L. Identification of factor-XIIIa-reactive glutamyl residues in the propolypeptide of bovine von Willebrand factor. *Eur J Biochem*. 1995;232:773–7.
- [55] Rawley O, Lillcrap D. Functional roles of the von Willebrand factor propeptide. *Hamostaseologie*. 2021;41:63–8.
- [56] Rawley O, Dwyer C, Nesbitt K, Notley C, Michels A, Lillcrap D. The VWF propeptide is a novel component of venous thrombi in a mouse model of DVT. *Res Pract Thromb Haemost*. 2022;6:(Abstract PB0802).
- [57] Swinkels M, Atiq F, Bürgisser PE, Moort I, Meijer K, Eikenboom J, Fijnvandraat K, Galen KPM, Meris J, Schols SEM, Bom JG, Cnossen MH, Voorberg J, Leebeek FWG, Bierings R, Jansen AJG, Fijnvandraat K, Coppens M, Meris J, Nieuwenhuizen L, et al. Platelet degranulation and bleeding phenotype in a large cohort of Von Willebrand disease patients. *Br J Haematol*. 2022;197:497–501.
- [58] Gralnick HR, Rick ME, McKeown LP, Williams SB, Parker RI, Maisonneuve P, Jenneau C, Sultan Y. Platelet von Willebrand factor: an important determinant of the bleeding time in type I von Willebrand's disease. *Blood*. 1986;68:58–61.
- [59] Fressinaud E, Baruch D, Rothschild C, Baumgartner H, Meyer D. Platelet von Willebrand factor: evidence for its involvement in platelet adhesion to collagen. *Blood*. 1987;70:1214–7.
- [60] Rodeghiero F, Castaman G, Ruggeri M, Tosetto A. The bleeding time in normal subjects is mainly determined by platelet von Willebrand factor and is independent from blood group. *Thromb Res*. 1992;65:605–15.

- [61] Kanaji S, Fahs SA, Shi Q, Haberichter SL, Montgomery RR. Contribution of platelet vs. endothelial VWF to platelet adhesion and hemostasis. *J Thromb Haemost.* 2012;10:1646–52.
- [62] Verhenne S, Denorme F, Libbrecht S, Vandenbulcke A, Pareyn I, Deckmyn H, Lambrecht A, Nieswandt B, Kleinschnitz C, Vanhoorelbeke K, De Meyer SF. Platelet-derived VWF is not essential for normal thrombosis and hemostasis but fosters ischemic stroke injury in mice. *Blood.* 2015;126:1715–22.
- [63] Bowman ML, Pluthero FG, Tuttle A, Casey L, Li L, Christensen H, Robinson KS, Lillicrap D, Kahr WHA, James P. Discrepant platelet and plasma von Willebrand factor in von Willebrand disease patients with p.Pro2808Leufs*24. *J Thromb Haemost.* 2017;15:1403–11.
- [64] Mannucci PM, Lombardi R, Bader R, Vianello L, Federici AB, Solinas S, Mazzucconi MG, Mariani G. Heterogeneity of type I von Willebrand disease: evidence for a subgroup with an abnormal von Willebrand factor. *Blood.* 1985;66:796–802.

SUPPLEMENTARY MATERIAL

The online version contains supplementary material available at <https://doi.org/10.1016/j.jtha.2023.03.041>